



# Numerical and Experimental Analysis of Remotely Pumped Dual-Function EDFA

Nadir Hossain\*, A.W. Naji, V. Mishra, F.M. Abbou, A.A.R. Hairul and A.R. Faizd

Institute of Photonics Research & Applications, Multimedia University,  
63100 Cyberjaya, Selangor, Malaysia.  
Email: nadir.hossain05@mmu.edu.my

**Abstract-** This paper presents a numerical analysis and experimental evaluation of remotely pumped Erbium doped fiber amplifier (EDFA) from the point of view of integrated attenuation and dispersion compensation inside the EDFA. Considering high gain and low noise figure (NF) by very low remote pump power as main design objective, the design process of remotely pumped optimized EDFAs for long haul optical fiber communication system (OFCS) is demonstrated. The effects of pump power, signal power, signal wavelength, EDF length and amplified spontaneous emission (ASE) on the gain and NF of remotely pumped EDFA are analyzed from the numerical simulation of EDFA rate equation model. Robustness and stability of the numerical model are shown by analyzing the output shapes using various design parameters. Finally, the numerical model is validated with the help of experimental results.

**Index Terms-** Dual-function, Erbium doped fiber amplifier, Long haul OFCS, Remote pump.

## I. INTRODUCTION

Remotely pumped EDFAs are attractive choice in long haul OFCS, where establishment of inline power stations are difficult, like undersea communication system. On the other hand chirped fiber Bragg gratings (CFBG) has been proven to be cost-effective dispersion compensating device because of its high dispersion figure of merit, lightweight, compact footprint, low cost and very low nonlinearity compared with conventional dispersion compensating fiber (DCF) module [1]. Dispersion compensation using EDFA integrated with a CFBG has been demonstrated

experimentally [2]. Because of the high importance of remotely pumped EDFA incorporated with a CFBG in modern long haul OFCS, a detailed analysis tool is essential to obtain the results of the system performance.

In order to maximize the efficiency of EDFA, the optimization of EDFA is necessary by optimizing its design parameters. Recently, experimental optimization techniques of EDFA have been reported [3, 4]. Pump power is optimized with respect to the optimized EDF length, in [3]. But optimum EDF length is dependent on the pump power. In case of remotely pumped EDFA, pump power is provided either from the transmitter or receiver side. Therefore, the main design objective is high gain and low NF using very low remote pump power. So, it is necessary to optimize the pump power before optimizing the EDF length. On the other hand, pump power is optimized with respect to a 5 meter long reference EDF, in [4]. But the length of reference EDF has noticeable effect on the optimization of pump power and hence there should be a guideline to select the length of reference EDF.

This paper focuses on the numerical analysis and experimental evaluation of remotely pumped EDFA incorporated with a CFBG to measure and analyze both attenuation and dispersion compensation inside the EDFA. A systematic approach towards attaining the design procedure of remotely pumped optimized EDFA using the numerical simulation of the EDFA rate equation model is described. This paper is organized as follows. Section II describes the remotely

pumped EDFA configuration followed by the rate equation model of EDFA in section III. Section IV presents the numerical simulation of the EDFA rate equation model. Section V describes the optimization of EDFA using numerical results. The robustness and stability of the numerical model are depicted in section VI. Experimental evaluation of numerical model is described in section VII. This paper concludes with a summary in section VIII.

## II. REMOTELY PUMPED EDFA CONFIGURATION

The basic configuration of remotely pumped EDFA integrated with a CFBG is depicted in Fig. 1. Forward pumping scheme with respect to the direction of input signal is considered to design the EDFA. A 980 nm pump provides higher gain and lower NF than a 1480 nm pump [5]. The EDFA designed in this work is for the remote pump application. Attenuation is higher for a 980 nm pump than a 1480 nm pump, therefore a 1480 nm remote pump is considered in this work which may provided either from the transmitter side (in case of remote post-amplifier) or receiver side (in case of remote pre-amplifier). The main noticeable device that is incorporated with the remotely pumped EDFA architecture is CFBG. It is utilized as a dispersion compensator to compensate the linear fiber dispersion just before the amplification of signal. For the purpose of numerical simulation, it is considered that, signal power launched from the transmitter is  $P_{Tx}^{out} = +10$  dBm. In case of remotely pumped long haul OFCS, the input signal power at the input of the EDFA is very low. If the input signal power to the EDFA is less than -40 dBm then the output amplified signal power from the EDFA does not provide an acceptable optical signal-to-noise ratio (OSNR) in the receiver. For this reason, during the optimization of EDFA using numerical simulation, operating signal power is considered approximately -35 dBm. In order to provide approximately -35 dBm input signal power to the EDFA, 225 km long span length between the

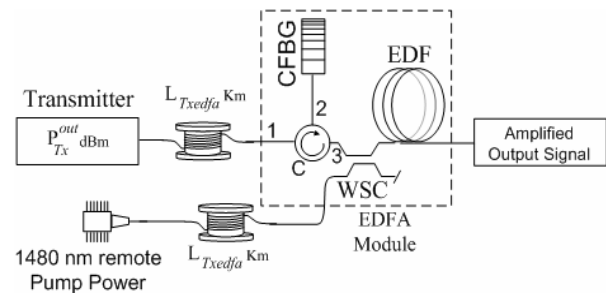


Fig. 1. Remotely pumped EDFA configuration.

transmitter to EDFA ( $L_{Txedfa}$ ) is considered. The span length may differ based on the launched signal power and fiber background loss of the transmission fiber. The transmission fiber is standard single mode fiber (SMF) with a mean dispersion of 17 ps/nm\*km and mean attenuation of  $\alpha = 0.20$  dB/km at 1550 nm signal wavelength. The CFBG considered in this work is fabricated to compensate the total dispersion of 1340 ps/nm. After traveling through the 225 km span length, the attenuated and distorted signal ( $P_{Scfbg}$ ) passed through the CFBG. During the dispersion compensation by the CFBG, signal is reflected by the CFBG, as a result there is a loss of signal due to the reflection. Reflection loss ( $R_{Loss}$ ) by the CFBG depends on the manufacturing process. For the purpose of numerical simulation,  $R_{Loss} = 10\%$  of the input signal in CFBG is considered in this work. The input signal ( $P_s$ ) of the port-1 of circulator (C) is output of port-2, which is entering as an input of the CFBG. After the dispersion compensation by the CFBG, the reflected signal from the CFBG enters as an input of port-2, which is the output of port-3. A wavelength selective coupler (WSC) is considered to combine the 1480 nm pump power with the output signal of port-3. The output of WSC enters as an input of the remotely pumped EDFA for the amplification of the signal.

## III. RATE EQUATION MODEL OF EDFA

The input signal power in the CFBG ( $P_{Scfbg}$ ) is calculated as:



$$P_{Scfbg} = P_{Tx}^{out} * e^{-\alpha L_{Edfa}} \quad (1)$$

The input signal ( $P_s$ ) at the beginning of the remotely pumped EDFA is calculated as:

$$P_s = P_{Scfbg} (1 - 0.01 * R_{Loss}) \quad (2)$$

Since the pumping at 1480 nm populates the upper amplifier level  $^4I_{13/2}$  of the Erbium ions directly, a two level transition between  $^4I_{15/2}$  -  $^4I_{13/2}$  is considered. It is assumed that the EDF medium is homogeneously broadened; ASE for polarization states as well as signal, pump and ASE are propagating in the fundamental mode. In order to concentrate on the remotely pumped EDFA fundamental characteristics, the system is simplified by neglecting the effects of excited state absorption (ESA), upconversion between Erbium ions, pair induced quenching, internal reflections due to discrete components and the Rayleigh back-scattering (RB) of the EDFA. The population densities  $N_1$  and  $N_2$  of the  $^4I_{15/2}$  and  $^4I_{13/2}$  are calculated as [6]:

$$N_1 = \rho \frac{1 + W_{21} \tau_{spon}}{1 + (W_{12} + W_{21}) \tau_{spon} + R \tau_{spon}} \quad (3)$$

$$N_2 = \rho \frac{R \tau + W_{12} \tau_{spon}}{1 + (W_{12} + W_{21}) \tau_{spon} + R \tau_{spon}} \quad (4)$$

Where  $W_{12}$  and  $W_{21}$  are the up and down stimulated transition rates respectively,  $R$  is the pumping rate,  $\tau$  is the fluorescence lifetime and by definition,  $\rho = N_1 + N_2$  is the Erbium ion density per unit volume.  $\sigma_{SE}(\lambda_s)$ ,  $\sigma_{SA}(\lambda_s)$ ,  $\sigma_{PE}(\lambda_p)$ ,  $\sigma_{PA}(\lambda_p)$  are the emission and absorption cross sections at signal ( $V_s$ ) and pump ( $V_p$ ) frequencies, respectively.  $\Gamma_s$  and  $\Gamma_p$  are the overlap factor, representing the overlap between the Erbium ions and the mode of the signal light field and pump light field respectively.  $A$  is the effective cross-sectional area of the distribution of Erbium ions.

The value of  $W_{12}$ ,  $W_{21}$  and  $R$  are calculated as:

$$W_{12} = \frac{\sigma_{SA}(\lambda_s) \Gamma_s}{h V_s A} [P_s + P_{ASE}^+ + P_{ASE}^-] \quad (5)$$

$$W_{21} = \frac{\sigma_{SE}(\lambda_s) \Gamma_s}{h V_s A} [P_s + P_{ASE}^+ + P_{ASE}^-] \quad (6)$$

$$R = \frac{P_p^+ \Gamma_p \sigma_{PA}(\lambda_p)}{h V_p A} \quad (7)$$

Where  $h$  is the Plank constant,  $P_p^+$  is the forward pump power as well as  $P_{ASE}^+$  and  $P_{ASE}^-$  are the forward and backward spontaneous emission spectrum. The equations describing the spatial development of  $P_s$ ,  $P_p^+$ ,  $P_{ASE}^+$  and  $P_{ASE}^-$  are written as based on the Giles and Desurvire model [7]:

$$\frac{dP_p^+}{dz} = P_p^+ \Gamma_p (\sigma_{PE}(\lambda_p) N_2 - \sigma_{PA}(\lambda_p) N_1) - \alpha_p P_p^+ \quad (8)$$

$$\frac{dP_s}{dz} = P_s \Gamma_s (\sigma_{SE}(\lambda_s) N_2 - \sigma_{SA}(\lambda_s) N_1) - \alpha_s P_s \quad (9)$$

$$\frac{dP_{ASE}^+}{dz} = \frac{P_{ASE}^+ \Gamma_s (\sigma_{SE}(\lambda_s) N_2 - \sigma_{SA}(\lambda_s) N_1)}{+ 2 \sigma_{SE}(\lambda_s) N_2 \Gamma_s h V_s \Delta v - \alpha_s P_{ASE}^+} \quad (10)$$

$$\frac{dP_{ASE}^-}{dz} = \frac{-P_{ASE}^- \Gamma_s (\sigma_{SE}(\lambda_s) N_2 - \sigma_{SA}(\lambda_s) N_1)}{+ 2 \sigma_{SE}(\lambda_s) N_2 \Gamma_s h V_s \Delta v + \alpha_s P_{ASE}^-} \quad (11)$$

Where  $z$  is the co-ordinate along the EDFA. The second term on the right hand side of equation (10) and (11) is the spontaneous noise power produced in per unit length of the EDFA within the EDFA homogeneous bandwidth ( $\Delta v$ ), for both polarization states.  $\alpha_p$  represents the internal pump loss term of the EDFA. NF is closely related to ASE, which is generated by spontaneous emission and the number of spontaneous photons is given by [5]:

$$\eta_{SP} = \frac{\eta N_2}{\eta N_2 - N_1} \quad (12)$$



Where  $\eta = \frac{\sigma_{SE}}{\sigma_{SA}}$ . The NF of remotely pumped EDFA ( $NF(\lambda_s)$ ) at the signal wavelength  $\lambda_s$  is calculated as:

$$NF(\lambda_s) = \frac{1+2\eta_{sp}[G-1]}{G} \quad (13)$$

Where  $G$  is the gain of remotely pumped EDFA. For high gain condition ( $G > 20$  dB) equation (13) is written as [6]:

$$NF(\lambda_s) \approx 2\eta_{sp} \quad (14)$$

#### IV. NUMERICAL SIMULATION OF EDFA RATE EQUATION MODEL

The first order differential equations (8)-(11) are two boundary value problem. Initially the integration of equations (8)-(11) is performed from  $z = 0$  to  $z = L$  using Runge-Kutta method neglecting  $P_{ASE}^-$  and considering  $P_p^+(z = 0) = P_{pinitial}^+$  (initial pump power to remotely pumped EDFA),  $P_s(z = 0) = P_s$  (initial signal power to remotely pumped EDFA) and  $P_{ASE}^+(z = 0) = 0$  as the initial boundary value. The whole set of equation including  $P_{ASE}^-$  are then integrated from  $z = L$  to  $z = 0$  using Runge-Kutta method with  $P_{ASE}^-(z = L) = 0$ . For the accuracy of these quasisolutions the same procedure is repeated using relaxation method to make iterative adjustment to the solution. The intrinsic parameters of EDF used to simulate the EDFA rate equation model is collected from the FIBERCORE Ltd, UK and shown in Table 1.

#### V. OPTIMIZATION OF EDFA USING NUMERICAL SIMULATION

At the beginning of this section, signal power and shape at the input of EDFA is calculated. A reference EDF is considered to start the optimization process. A guideline to select the length of reference EDF is described. The

Table 1: EDF parameters used in simulation

Parameter	Value
$\lambda_s$	1550 nm.
$\lambda_p$	1480 nm.
$\Gamma_s$	0.74
$\Gamma_p$	0.77
$A$	$1.633 \times 10^{-11} \text{ m}^2$
$\rho$	300 ppm
$\alpha_s$	0.20 dB/Km
$\sigma_{SA}(\lambda_s)$	$2.910556003 \times 10^{-25} \text{ m}^2$
$\sigma_{SE}(\lambda_s)$	$4.118853202 \times 10^{-25} \text{ m}^2$
$\sigma_{PA}(\lambda_p)$	$2.787671233 \times 10^{-25} \text{ m}^2$
$\sigma_{PE}(\lambda_p)$	$0.810563905 \times 10^{-25} \text{ m}^2$
$\Delta v$	3100 GHz (25 nm)
$\tau_{spont}$	0.0102 seconds
$\alpha_p$	0.24 dB/Km

operating pump power is optimized with respect to the reference EDF of selected length. The length of EDF is then optimized by two ways. First, by calculating  $N1$  and  $N2$  as a function of position along the length of EDFA. Second, by calculating the gain as a function of EDF length. Both ways show the same optimized length. The relation between the EDF length, ASE and EDFA gain is described. EDFA is characterized by calculating gain as a function of signal wavelength by various pump powers. Finally, the effect of dispersion compensation inside the EDFA is described at the end of this section.

During the transmission through the 225 km span length between the transmitter to amplifier,  $P_{Tx}^{out} = +10$  dBm is attenuated and distorted and hence  $P_{Scfbg} = -35$  dBm. Fig. 2 shows  $P_{Tx}^{out}$ , distorted signal after traveling the 225 km span length between the transmitter to EDFA as well as dispersion compensated signal using a CFBG. Total dispersion of signal due to the transmission through the 225 km transmission fiber is 3825 ps/nm. The CFBG has an internal reflection loss of 10% of the input signal and

compensates a total dispersion of 1340 ps/nm. Therefore, the input signal power to the EDFA ( $P_s$ ) is -35.46 dBm and it has a dispersion of 2485 ps/nm.

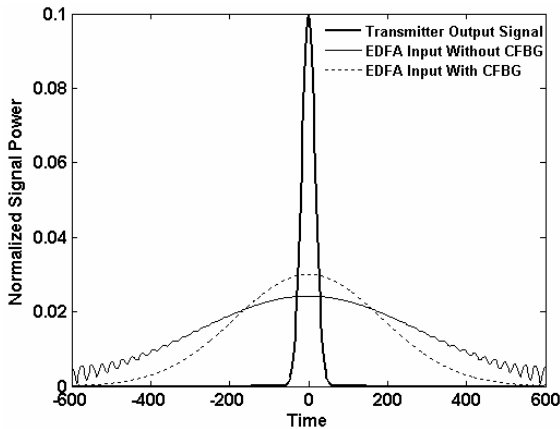


Fig. 2. Launched signal power from the transmitter as well as signal with and without dispersion compensation using a CFBG before amplification, as a function of time.

In case of remotely pumped EDFA, location of the EDFA is far away from the pump source and for this reason the necessity of very low operating pump power is essential. At the beginning of the optimization, a reference EDF is considered. Gain, NF, threshold and saturation pump power characteristics of EDFA are analyzed by varying the length of reference EDF. It is found that, if the length of reference EDF is shorter than 10 meter, EDFA is saturated by very low pump power and provides low gain. For example, using a 5 meter long reference EDF, the EDFA is saturated by only 7 mW pump power and provides 5.59 dB gain only. On the other hand, the EDFA of length 10 to 18 meter shows almost same saturation characteristics and saturated by 14 mW remote pump power, although total gain and NF are not same for different lengths. If the length of reference EDF is longer than 18 meter, then threshold and saturation pump power is become higher. For example, using a 40 meter long reference EDF, the EDFA threshold pump power is 9.5 mW and saturated by very high 35 mW pump power. The main design objective of

the remotely pumped EDFA is high gain and low NF using very low remote pump power. Though using longer EDF and higher operating pump power, the EDFA is able to provide a high gain, but the use of high remote pump power conflicts with the main design objective of remotely pumped EDFA. So any length within 10-18 meter can be selected as a reference length for the EDF mentioned in Table 1.

A 10 meter long EDF is selected as a reference for the current work. The gain and NF characteristics at 1550 nm as a function of pump power using a 10 meter long EDF is shown in Fig. 3. Referring to the Fig. 3, for the increment of pump power from 5 to 14 mW, signal gain increases from 8.73 to 12.02 dB and NF decreases from 5.49 to 4.65 dB. On the other hand, for the increment of pump power from 14 to 60 mW, signal gain increases from 12.02 to 13.54 dB and NF decreases from 4.65 to 4.35 dB. These results clearly show that the increment of gain and the decrement of NF are very low with respect to the increment of pump power exceeding 14 mW. Therefore, the pump power of 14 mW is chosen as the optimum pump power, because pump power exceeding 14 mW has not high impact on the gain and NF of 10 meter long EDFA.

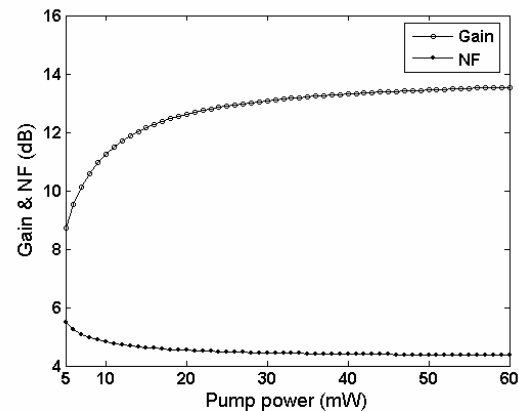


Fig. 3. Gain and NF in dB as a function of pump power in mW using a 10 meter long reference EDF at 1550 nm signal wavelength and injected signal power of -35.46 dBm.

The length of EDFA is optimized numerically by calculating the  $N_2$  and  $N_1$  as a function of

position along the length of EDFA by varying the EDF length against the operating pump and signal power. It is found that, if the length of EDF is shorter than 21 meter, at the end of EDFA pump power is higher than the threshold power and hence  $N1$  and  $N2$  curves do not intersect each other. For example, using a 15 meter long EDFA,  $N1$  and  $N2$  at the end of EDFA is  $6.1786 \times 10^{23}$  and  $1.9084 \times 10^{24}$  ions per cubic meter, respectively. These results show that, at the end of 15 meter long EDFA  $N2$  is substantially higher than the  $N1$  and hence  $N1$  and  $N2$  curves do not intersect each other. On the other hand, if the length of EDF is 21 meter, available pump power at the end of EDFA is less than the threshold pump power which is not able to invert the population in the additional length of EDF exceeding 21 meter. As a result,  $N1$  and  $N2$  curves intersect each other at the end of the 21 meter long EDFA, as shown in Fig. 4. It is also found that, if an EDF of length more than 21 meter is used then the portion of the EDF that exceeds 21 meter remains unpumped. This unpumped portion of the EDF absorbs the signal and degrades the EDFA performance.

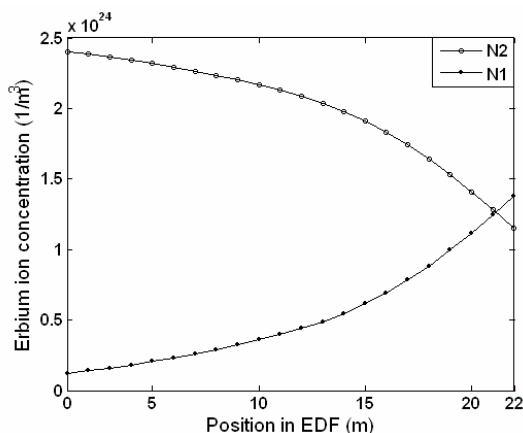


Fig. 4. Population in the upper state ( $N2$ ) and ground state ( $N1$ ) as a function of position along a 21 meter long EDF at 1550 nm using 14 mW of pump power and injected signal power of -35.46 dBm.

The length of EDFA is also optimized by calculating the gain as a function of EDF length against the operating pump and signal power. Fig. 5 shows gain as a function of EDF length by 14 mW remote pump power and injected

signal power of -35.46 dBm. Referring to the Fig. 5, 19.08, 19.32, 19.51, 19.47 and 19.40 dB gain are obtained using 19, 20, 21, 22 and 23 meter long EDF, respectively. These results clearly show that the gain increases up to the length of 21 meter and after the 21 meter it begins to reduce again. Due to the absorption of pump power along the EDF, portion of the EDF that exceeds 21 meter is remained unpumped. This unpumped portion of EDF absorbs the signal instead of the amplification of signal. Overall EDFA gain is achieved by the cumulative gain through the whole EDF length. Although signal is amplified up to 21 meter but the absorption of signal after the 21 meter causes the degradation of EDFA performance by the reduction of cumulative gain which justifies the findings in Fig. 4.

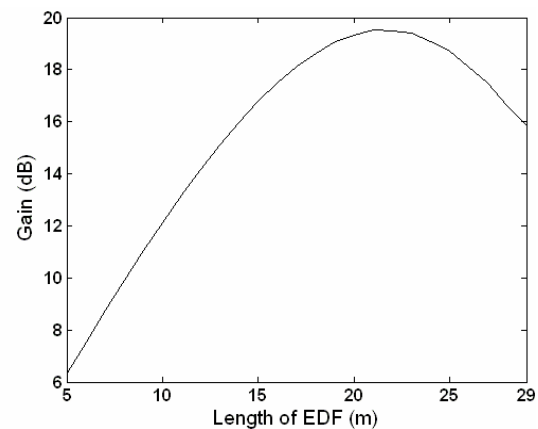


Fig. 5. Gain as a function of EDF length at 1550 nm signal wavelength using 14 mW of pump power and injected signal power of -35.46 dBm.

The ASE has a noticeable effect on the total gain of the EDFA. It is found that, if an EDF of length more than 21 meter is used, because of the additional length of EDF, backward ASE travels over a longer distance and become much higher at the beginning of the EDFA which depletes the inversion and robs gain at the expense of the signal. For example, Fig 6(a) and 6(b) shows the forward and backward traveling ASE as a function of position along a 21 and 29 meter long EDFA, respectively. Referring to the Fig 6, backward ASE at the beginning of 29 meter long EDFA is  $4.43 \times 10^{(-2)}$  mW, which

is  $2.60 \times 10^{-2}$  mW higher than the 21 meter long EDFA. On the other hand, if an EDF of length less than 21 meter is used then a portion of the pump power remains unused which causes more population inversion and hence the increment of the gain. For these reasons, a 21 meter long EDF is chosen as the optimum length using 14 mW remote pump power against the signal power of -35.46 dBm for the EDF mentioned in Table 1.

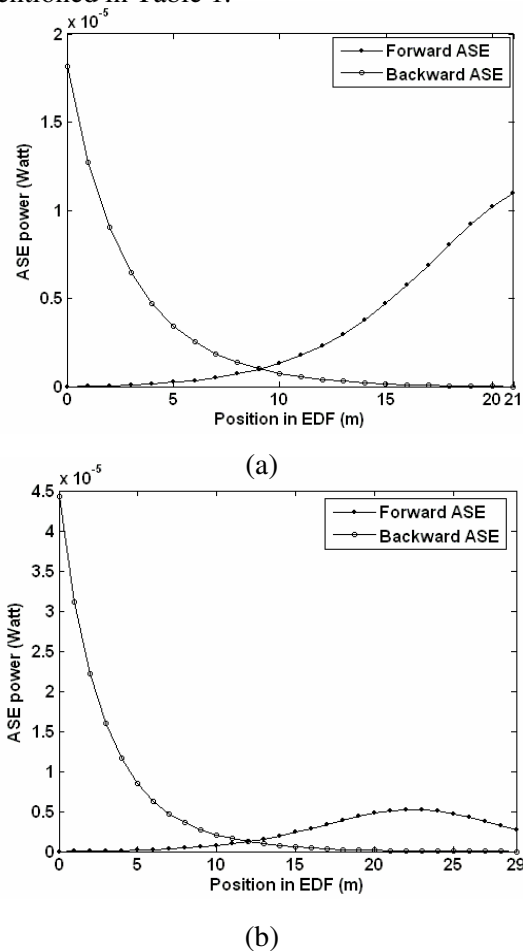


Fig. 6. Forward and backward ASE as a function of position along a 21 meter long EDF (Fig. 6(a)) and 29 meter long EDF (Fig. 6(b)) at 1550 nm signal wavelength using 14 mW of pump power and injected signal power of -35.46 dBm.

Generally the long haul OFCS is a multi-channel system which may uses the signal of several wavelengths. For the purpose of numerical simulation as well as demonstrate the

optimization and experimental evaluation of EDFA only signal of 1550 nm wavelength is considered. But the EDFA rate equation model is also simulated using a range of wavelengths (1520-1560 nm) by selecting the corresponding absorption and emission cross sections of each wavelength, to characterize the gain performance of multi-channel system. Fig. 7(a) shows the absorption and emission cross sections of Erbium near 1500 nm for the EDF mentioned in Table 1, which are collected from the FIBERCORE Ltd., UK. These cross sections are used to simulate the remotely pumped EDFA. Fig. 7(b) shows the gain in dB as a function of signal wavelength for various pump powers and injected signal power of -35.46 dBm using a 21 meter long EDF.

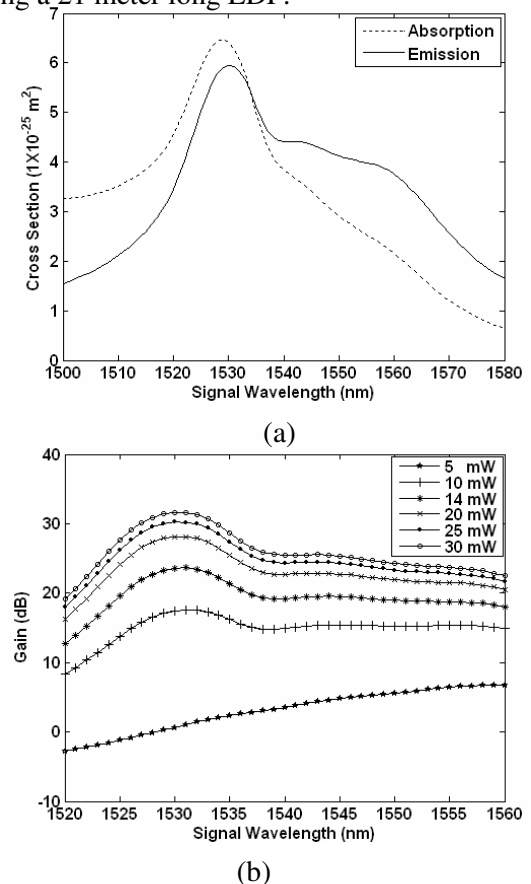


Fig. 7. Absorption and emission cross sections of Erbium near 1500 nm (Fig. 7(a)) and gain in dB as a function of signal wavelength for various pump powers and injected signal power of -35.46 dBm using a 21 m long EDF (Fig. 7(b)).

Referring to the Fig. 7(b), maximum gain is obtained at 1530 nm due to its higher emission cross section. The spectral shapes of the gain change nonuniformly with the changes in pump power. In particular, as pump power decreases, signals near 1530 nm will experience a drop in gain much more significant than that for signals near 1550 nm as shown in Fig 7(b).

Fig. 8 shows the amplified signal from the output of the remotely pumped EDFA without dispersion compensation and with dispersion compensation using CFBG before the amplification of signal. Referring to the Fig 8, amplified signal with dispersion compensation has higher signal intensity than the amplified signal without dispersion compensation. This result clearly shows that, an EDFA integrated with CFBG provides amplified signal with higher intensity as well as reshapes the distorted signal inside the EDFA.

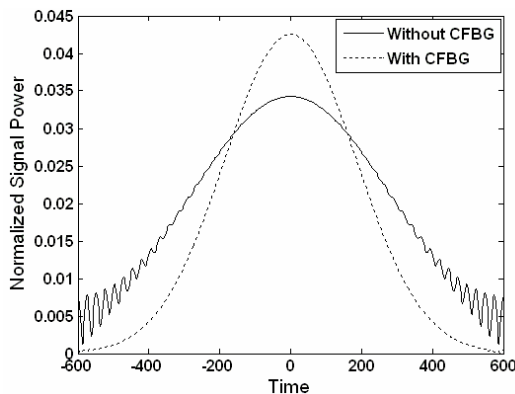
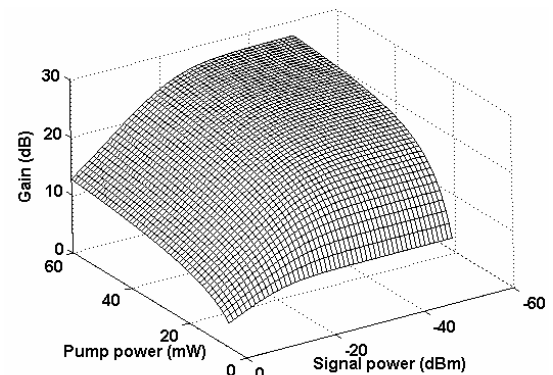


Fig. 8. Amplified signal as a function of time with and without dispersion compensation using a CFBG at the beginning of EDFA.

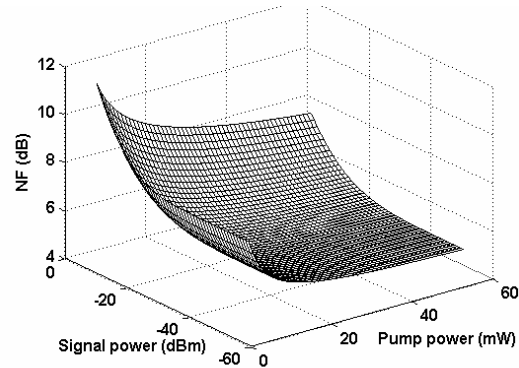
## VI. ROBUSTNESS AND STABILITY OF THE NUMERICAL MODEL

The main purpose of the numerical simulation of EDFA rate equation model in this work is to help the designers to carry out the design of an optimized EDFA for long haul OFCS. Therefore, the model should show the same output characteristics or numerical results for any input signal and pump power. Fig. 9 shows the gain (Fig. 9(a)) and NF (Fig. 9(b)) in dB as a function of pump power in mW and signal

power in dBm using a 21 meter long EDF at 1550 nm signal wavelength. From the Fig. 9(a), gain values are gradually increased with the increment of pump power. This is because, the increment of pump power increases the upper state population as well as inverts the more length of the EDF. As a result gain increases due to the increment of the Erbium ions population inversion and higher EDF length increases the total cumulative gain. Fig. 9(a) also shows that the gain values are gradually decreased with the increment of signal power because the pump can no longer replenish the inversion as fast as the signal depletes it.



(a)



(b)

Fig. 9. Gain (Fig. 9(a)) and NF (Fig. 9(b)) in dB as a function of pump power in mW and signal power in dBm using a 21 m long EDF at 1550 nm signal wavelength.

Referring to the Fig. 9(b), NF drops smoothly as the pump power is increased. This is because with the increment of pump power, population inversion becomes higher and strong backward



signal get more amplification. On the other hand, length of the EDF is optimized for the EDFA and hence backward ASE are not strong enough to significantly affect the inversion at the input of the fiber; as a result NF drops smoothly. Fig. 9(b) also shows that the NF increase dramatically with the increment of signal power. At higher input signal power levels, the strong signal significantly depletes the Erbium ions inversion and the pump is not able to replenish it as a result the NF increase rapidly with signal power. Finally, Fig. 9 clearly shows that the numerical results of the EDFA have same characteristics for any input pump and signal power. The smoothness of the 3D shape shows the similarity between the numerical results by any input signal and pump power. So the numerical model is stable and robust, which is able to help the designers to carry out the design of optimal EDFA to be used in long haul OFCS.

## VII. EXPERIMENTAL EVALUATION OF THE NUMERICAL MODEL

Experimental work is carried out and reported in [3]. The EDF, which is used in the experiment has  $\rho = 440$  ppm,  $A = 19.8 \times 10^{-12} \text{ m}^2$ ,  $\Gamma_s = 0.40$ ,  $\Gamma_p = 0.43$ ,  $\sigma_{sa}(\lambda_s) = 2.85 \times 10^{-25} \text{ m}^2$ ,  $\sigma_{se}(\lambda_s) = 4.03 \times 10^{-25} \text{ m}^2$ ,  $\sigma_{pa}(\lambda_p) = 2.86 \times 10^{-25} \text{ m}^2$ ,  $\sigma_{pe}(\lambda_p) = 0.42 \times 10^{-25} \text{ m}^2$  and  $\tau = 0.01$  seconds. The operating pump power of the EDFA is 10 mW from the 1480 nm pump source, length of the EDFA is 13.5 meter and operating signal power is varied from -40 to -10 dBm at 1550.3 signal wavelength. The rate equation model of EDFA is simulated using these parameters and obtained numerical results are compared with the experimental results, as shown in Fig. 10. Referring to the Fig. 10, gain and NF curves obtained from numerical simulation as well as experimental results have the similar shape. Numerical results show more gain and less NF than the experimental results. This is due to the splicing losses of EDF which is neglected during the numerical simulations. Also the effects of excited state absorption (ESA), upconversion between Erbium ions, pair induced quenching, internal reflections due to

discrete components and the Rayleigh back-scattering (RB) of the EDF is neglected during the numerical simulation which may reduce the gain during the experimental work.

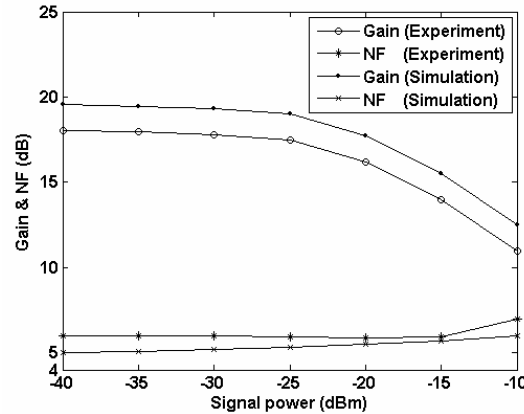


Fig. 10. Comparison between the numerical simulation and experimental results reported in [3].

## VIII. CONCLUSION

The physical base of remotely pumped EDFA integrated with a CFBG is described. A combination of Runge-Kutta and relaxation method is used to numerically solve the EDFA rate equation model. The numerical results are used to describe the design procedure of remotely pumped optimized EDFA. At the beginning of the optimization a reference EDF is considered. A guideline to select the length of reference EDF is depicted. Optimization of the pump power and EDF length is demonstrated. The effects of pump and signal power, signal wavelength, EDF length and ASE on the gain and NF of the remotely pumped EDFA are analyzed. The robustness and stability of the numerical results are shown by analyzing the output shape by various input signal and pump power. Finally, the numerical results are validated with the help of experimental results and intrinsic parameters of the same EDF. These numerical results will play an important role to the design of practical optimized EDFAs for the long haul OFCS from the point of view of economic usage of pump power, optimal use of EDF and integrated attenuation and dispersion compensation inside the EDFA.

## ACKNOWLEDGEMENT

The authors wish to thank the application engineers of FIBERCORE Ltd, UK for the EDF parameters and all the members of Institute of Photonics Research & Applications (IPRA), Multimedia University, Malaysia for helpful discussion.

## REFERENCES

- [1] T. Zhi, J. Shui-Sheng, W. Guang-Quan, C. Hong, L. Ju-Hao, Z. Lei, C. Zhang-Yuan, W. Zi-Yu, Z. Li-Xin, X. An-Shi, H. Guang-Ming, Z. Ya-Ming, W. Huai, N. Ti-Gang, L. Yan, and T. Zhong-Wei, "Ultra-long haul L-band WDM transmission over a standard single mode fiber using DCF + CFBG hybrid dispersion compensation", *Chinese Physics Letter*, vol. 23, no. 2, pp. 392-395, 2006.
- [2] M. Z. Jamaludin, A. A. A. Bakar, A. W. Naji, F. A. Rahman, M. A. Mahdi, and M. K. Abdullah, "Improving the performance of double-pass EDFA utilizing chirped bragg grating as feedback loop", *MICROWAVE AND OPTICAL TECHNOLOGY LETTERS*, vol. 48, pp. 386-388, 2006.
- [3] A. W. Naji, M. S. Z. Abidin, M. H. Al-Mansoori, M. Z. Jamaludin, M. K. Abdullah, S. J. Iqbal, and M. A. Mahdi, "Dual-function remotely-pumped Erbium-doped fiber amplifier: Loss and dispersion compensator", *OPTICS EXPRESS*, vol. 14, no. 18, pp. 8054-8059, 2006.
- [4] A. W. Naji, M. S. Z. Abidin, M. H. Al-Mansoori, M. Z. Jamaludin, M. K. Abdullah, S. J. Iqbal, M. K. Abdullah, and M. A. Mahdi, "Double-Pass Remotely Pumped  $\text{Er}^{3+}$ -Doped Fiber Amplifier Embedded with Chirped Fiber Bragg Grating", *MICROWAVE AND OPTICAL TECHNOLOGY LETTERS*, vol. 48, no. 10, pp. 1993-1996, 2006.
- [5] P. C. BECKER, N. A. Olsson, and J. R. Simpson, *Erbium-Doped Fiber Amplifiers*. NY: Academic Press, 2002.
- [6] E. Desurvire, *Erbium-Doped Fiber Amplifiers*. NY: John Wiley & Sons, Inc, 1994.
- [7] C. R. Giles, and E. Desurvire, "Propagation of Signal and Noise in Concatenated Erbium Doped Fiber Optical Amplifiers", *IEEE Journal of Lightwave Technology*, vol. 9, no. 2, pp. 147-154, 1991.